Extensive Scaling from Computational Homology and Karhunen-Loève Decomposition Analysis of Rayleigh-Bénard Convection Experiments

Hüseyin Kurtuldu, Konstantin Mischaikow, and Michael F. Schatz

Phys. Rev. Lett. **107**, 034503 — Published 14 July 2011

DOI: 10.1103/PhysRevLett.107.034503

Extensive scaling from computational homology and Karhunen-Loève decomposition analysis of Rayleigh-Bénard convection experiments

Hüseyin Kurtuldu,[1] Konstantin Mischaikow,[2] and Michael F. Schatz[1]
[1] *Center for Nonlinear Science and School of Physics, Georgia Institute of Technology, Atlanta, Georgia 30332, USA and*
[2] *Department of Mathematics, Rutgers University, New Jersey 08854, USA*
(Dated: May 9, 2011)

Spatio-temporally chaotic dynamics in laboratory experiments on convection are characterized using a new dimension, $D_{\rm CH}$, determined from computational homology. Over a large range of system sizes, $D_{\rm CH}$ scales in the same manner as $D_{\rm KLD}$, a dimension determined from experimental data using Karhuenen-Loéve decomposition. Moreover, finite-size effects (the presence of boundaries in the experiment) lead to deviations from scaling that are similar for both $D_{\rm CH}$ and $D_{\rm KLD}$. In the absence of symmetry, $D_{\rm CH}$ can be determined more rapidly than $D_{\rm KLD}$.

PACS numbers:

Characterizing data from experiments on spatially extended non-equilibrium systems is a challenge [1]. Methods devised to extract information from low-dimensional systems [2] fail as the number of dynamical degrees of freedom (DOF) increases. Recently, methods have been developed to determine the number of DOF in numerical simulations [3–8]; these methods suggest that the already large number of DOF grow still larger as the system size increases, i.e, the number of DOF in spatially extended systems is an extensive quantity. The techniques for measuring the number of DOF in simulations require very precise control of the initial conditions and, therefore, cannot be used in most experimental systems. What are needed are good, experimentally accessible methodologies to characterize the number of DOF efficiently in large experiment data sets not only to measure how DOF scale with system size, but also to detect the impact of finite size effects (always present in experiments) on the behavior of the number of DOF.

In this letter, we show, for the first time, that the impact of finite size effects on the dynamics of a spatio-temporally chaotic system can be characterized quantitatively. This characterization was performed in two very different methods: (1) By using the well-established pattern characterization tool, Karhunen-Loève decomposition(KLD) [9] to compute the KLD dimension $D_{\rm KLD}$ [10], and (2) by applying the tools of algebraic topology (computational homology) [11] to compute a novel topological dimension $D_{\rm CH}$ (defined below). Both measures of dynamical dimension not only show the system is extensively chaotic but also exhibit the same *quantitative* deviation from scaling due to the presence of system boundaries. This suggests our approach to describing finite-size effects should be independent of the particular method used to characterized the dimensionality of the dynamics.

Computational homology (CH) based on algebraic topology is a metric-independent characterization technique that aims to measure the complexity of the geometry of the structures in high-dimension systems [11]. Homology computations, in an N dimensional topological space X, produce a set of N non-negative integers $\beta_k(X)$ ($k = 0, 1, \ldots, N-1$) known as Betti numbers. Each $\beta_k(X)$ characterizes a unique topological property of X and a set of Betti numbers provides a reduced description for X. Two distinct, two-dimensional topological spaces can be obtained from each shadowgraph image (Fig. 1) of spatio-temporally chaotic convective flow; specifically, image pixels whose intensity are lower (higher) than the median intensity for a given image belong to the cold (hot) topological space X_c (X_h). Homology computations yield two characteristic Betti numbers for each space: β_{0c} (β_{0h}) which counts the number of distinct connected cold (hot) components and β_{1c} (β_{1h}) which counts the number of cold (hot) holes formed within X_c (X_h). Alternatively, β_{1c} (β_{1h}) counts the number of hot (cold) connected regions completely surrounded by cold (hot) flow. We use the quartet $\{\beta_{0c}, \beta_{1c}, \beta_{0h}, \beta_{1h}\}$ to define the CH state of the convection pattern at the instant of time when the pattern's image is recorded. The time evolution of CH states is characterized by successive computations of Betti numbers from a time series of images; the number of distinct CH states are counted, thereby, yielding an estimate of p_k, the probability of occurrence for a given state. We introduce a positive integer $D_{\rm CH}$ as a function of f:

$$D_{\rm CH} \;=\; \min\left\{k : \sum_{k=1}^{k+1} p_k > f\right\} \qquad (1)$$

which defines the minimum number of CH states k needed to capture some fraction $f \leq 1$ of the total probability. Here, we use $D_{\rm CH}$ to measure the spatio-temporal disorder of an extensively chaotic experimental system.

KLD analysis is widely used to extract important dynamical modes from data sets. To analyze shadowgraph data using KLD, an ensemble of space-time data $\boldsymbol{u}(\boldsymbol{x}, t)$ is first formed from the intensity arrays $\boldsymbol{u}(\boldsymbol{x_i}, t_j)$, which represent the pixel value recorded at position $\boldsymbol{x_i}$ at time t_j. The eigenvectors as KLD modes with associated

eigenvalue λ are generally obtained from an eigendecomposition of the tensor $< \boldsymbol{u}(\boldsymbol{x},t)\otimes\boldsymbol{u}(\boldsymbol{x'},t) >$, which is built by the two-point correlation of the elements of $\boldsymbol{u}(\boldsymbol{x},t)$ averaged over time [9]. Conventional KLD algorithms are computationally intensive on large data sets and generally done using a singular value decomposition and hence is of order n^3 where n is the number of pixels in both space and time. In order to overcome this problem we implement a modified KLD algorithm proposed by Duggleby and Paul [12] for numerical data that exploits the azimuthal symmetry for a rotationally invariant experimental system. This results in a small eigenvalue problem; for each wavenumber n one must analyze the tensor $< \hat{\boldsymbol{u}}_n(r,t) \otimes \hat{\boldsymbol{u}}_n^*(r',t) >$, where $\hat{\boldsymbol{u}}_n(r,t)$ is the Fourier transform of $\boldsymbol{u}(\boldsymbol{x},t)$ in the azimuthal direction and $*$ denotes the complex conjugate. In computations the eigenvalues are arranged in descending order and normalized by the sum of all the eigenvalues. The KLD dimension $D_{\rm KLD}$ [10]

$$D_{\rm KLD} \;=\; \min\left\{ m : \sum_{m=1}^{m+1} \lambda_m > f \right\} \qquad (2)$$

defines the minimum number of KLD modes m required to capture some fraction $f \leq 1$ of the total eigenvalue spectrum. A numerical study by Zoldi and Greenside [10] on a homogeneous extended chaotic system showed that the Lyapunov dimension D_λ (the number of dynamical DOF captured by the Lyapunov exponents [2]) and $D_{\rm KLD}$ demonstrate analogous extensivities. D_λ and $D_{\rm KLD}$ scale linearly at similar rates with either size (area) of the entire system or size of a sufficiently large subsystem in a fixed system size.

Rayleigh Bénard convection (RBC) of a horizontal fluid layer heated from below is considered a paradigm to investigate the nature of pattern formation, and has motivated numerous numerical and laboratory studies [13]. We study RBC experimentally in a cylindrical convection cell of aspect ratio $\Gamma \equiv r_0/d$ (radius to depth ratio) in which a compressed gas is confined. A similar set up is described in detail by de Bruyn et al. [14]. Patterns of convective flows are acquired by controlling the reduced Rayleigh number $\epsilon = (\Delta T - \Delta T_c)/\Delta T_c$ above the onset of convection that occurs at a critical temperature difference ΔT_c between top and bottom of the cell. We analyze the convection in the state known as spiral defect chaos (SDC) [15]. In order to study extensivity in SDC, four large sets of spatio-temporally chaotic data are acquired in different experiments as described in Table I. D-I and D-III are taken in two different Γ cells where gaseous CO_2 is bounded by a lateral wall made of filter paper. D-II is obtained in the same cell with gaseous SF_6 while D-IV is acquired in an experiment performed with SF_6 and a plastic (polyethersulfone) sidewall [19]. The thermal conductivities of the paper and of the plastic walls are, respectively, about a factor of 4 and 10 times larger than the thermal conductivity of the fluid used. Sample patterns are shown in Fig. 1.

DATA	Γ	Fluid	Sidewall	Pr	t/t_h	$N/10^3$
D-I	35	CO_2	Paper	0.98	451	100
D-II	35	SF_6	Paper	0.87	20	3
D-III	30	CO_2	Paper	0.98	50	15
D-IV	30	SF_6	Plastic	0.95	130	105

TABLE I: SDC data taken in four different experimental cells at $\epsilon = 0.8$ with the aspect ratio Γ, the fluid and the sidewall used. Pr is the Prandtl number and t is the observation time in units of the horizontal diffusion time $t_h = \Gamma^2 t_v$. The vertical diffusion time t_v is order of seconds. N is the number of images captured for computations.

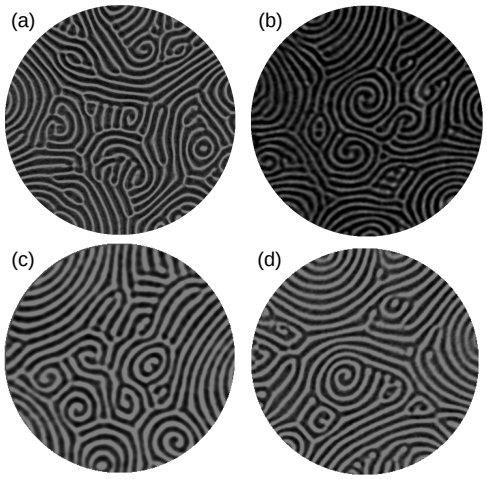

FIG. 1: Shadowgraph patterns of SDC at $\epsilon = 0.8$ (a) from D-I (b) from D-II, (c) from D-III and (d) from D-IV. Bright and dark regions represent hot and cold flows respectively. The median value of intensity in an image is used as a threshold value to form two distinct binary images that represent topological spaces for hot X_h and cold flows X_c, respectively. Homology analysis yields the following topological states for the entire patterns, $\{\beta_{0c}, \beta_{1c}, \beta_{0h}, \beta_{1h}\}$: (a) $\{64, 2, 29, 13\}$, (b) $\{61, 4, 35, 6\}$, (c) $\{42, 3, 28, 8\}$ and (d) $\{43, 4, 44, 4\}$ see Ref. [16] for more details.

CH and KLD provide very different methods for analyzing convection patterns; nevertheless, we find $D_{\rm KLD}$ and $D_{\rm CH}$ increase in a similar manner as new degrees of freedom are added. We explore extensivities of $D_{\rm KLD}$ and $D_{\rm CH}$ for different subsystems sizes in D-I, which are obtained by sampling the data spatially with a circular window of increasing radii r, measured in units of depth d from the cell center. We work with a fixed fraction $f = 0.7$ [17] to compute $D_{\rm KLD}$ and $D_{\rm CH}$ from the eigenvalue spectra and the probability distributions, respectively, for each subsystem. We find that, over a large range of subsystem sizes, $D_{\rm KLD}$ scales extensively with the area of the system $A \propto r^2$ (Fig. 2), consistent with the results of KLD analyses in previous numerical and

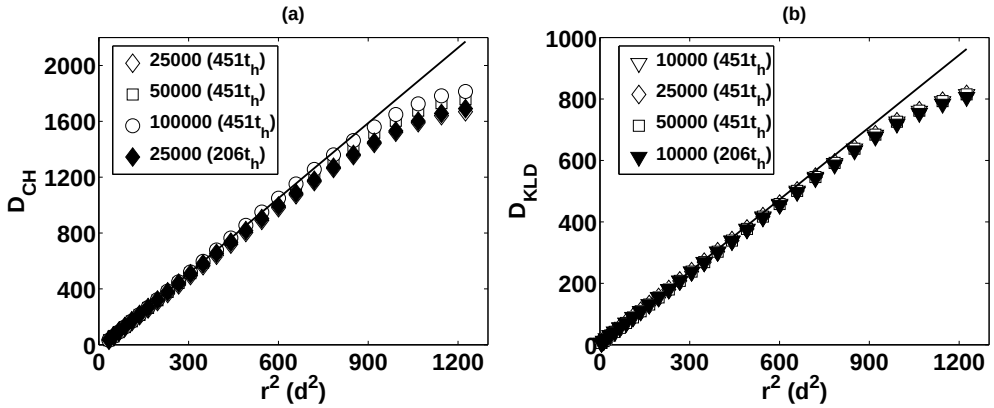

FIG. 2: Extensive scalings of $D_{\rm CH}$ and $D_{\rm KLD}$ for increasing subsystem sizes are obtained by computational homology (a) and a modified KLD algorithm based on a Fourier method (b), respectively for fraction $f = 0.7$ in D-I. The number of images, at given observation times, used at each data point in computations is labeled. The linear lines are drawn to guide the extensitivies to eye. Choosing f very close to 1 may include experimental errors, whereas choosing it too small may exclude necessary modes and states necessary to describe the dynamics. But, for the range $0.5 \leq f \leq 0.9$, extensive scalings of dimensions normalized by the maximum dimension at each f nearly fall on a single curve.

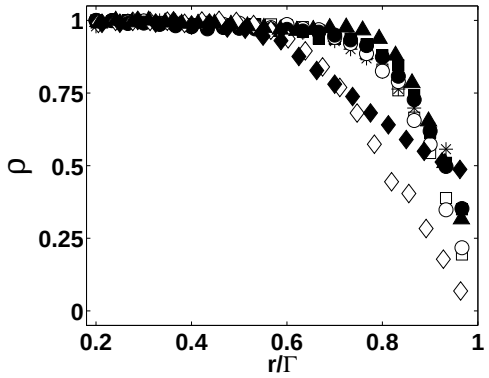

FIG. 3: The rates of increase ρ estimated from extensive scalings of $D_{\rm CH}$ (open symbols) and $D_{\rm KLD}$ (closed symbols) are shown as a function of r/Γ in units of cell depth d to indicate the sidewall effects in the experiments, D-I (squares), D-II (triangles), D-III (circles), D-IV (diamonds), at $\epsilon = 0.8$. ρ is only calculated from $D_{\rm KLD}$ in D-II. While D-I, D-II, and D-III are performed with a paper sidewall, D-IV is conducted with a plastic boundary. The number of images used for computations in D-I, D-II, D-III and D-IV is given in Table I. Also, ρ as dimension per area is obtained from the conventional KLD algorithm (asterisks) by sampling the data of $10,000$ images in D-I with an annular window of inner r and outer $r + 2d$ radius ($r \geq 7d$).

experimental studies that strongly suggest that the state of SDC is extensively chaotic [10, 17]. We find that $D_{\rm CH}$ also provides strong evidence for extensive chaos; $D_{\rm CH}$ also scales extensively with r^2 over substantially the same broad range of subsystem sizes as $D_{\rm KLD}$ (Fig. 2).

Computational homology offers a way to measure dimensions that converges more rapidly than dimensions measured using KLD. Conventional KLD become prohibitively expensive to compute even for moderately large system sizes; as a result, measurements of $D_{\rm KLD}$ can fail to converge [17]. Fourier-based KLD (used in our analysis) provides faster and converged estimates of $D_{\rm KLD}$ in large subsystem sizes [12]; it is, however, only suitable for systems with rotational or translational invariance. CH has no such limitations and can be performed on sufficiently large systems with a boundary of any shape. It is far easier to compute $D_{\rm CH}$ than $D_{\rm KLD}$ since the CH analysis is carried out separately for each snapshot.

We demonstrate the convergence for both KLD and CH analyses of our data by using different sampling methods. In one approach, we change the sampling rate, thereby changing both total observation time and the number of images in the analysis. We find both $D_{\rm KLD}$ and $D_{\rm CH}$ converge provided that sufficiently large data sets are used in computations (Fig. 2). We also compute extensive scaling of $D_{\rm CH}$ by using samples randomly chosen from the data; $D_{\rm CH}$ exhibits exactly the same scaling with the subsystem sizes in data sets of $25,000$ images selected either randomly or a fixed sampling period of $451t_h$.

As the analyzed subsystem size approaches the physical size of the experiment, both $D_{\rm CH}$ and $D_{\rm KLD}$ deviate from scaling in the same way (Fig. 3). To compare this deviation in both dimensions quantitatively, we use an intensive quantity $\rho = \partial D/\partial A$ measured as a function of the radial distance from the cell center. For each dimension, the values of ρ are normalized to remove parametric dependence on the choice of f; moreover, the radial distance r is normalized by the aspect ratio Γ. In this representation (Fig. 3), $\rho = 1$ (for small r/Γ) indicates both $D_{\rm CH}$ and $D_{\rm KLD}$ scale linearly with the area; however, ρ becomes significantly less than one for both $D_{\rm CH}$ and $D_{\rm KLD}$ for r/Γ sufficiently large. Remarkably, the deviation of ρ from unity exhibits a similar functional

dependence on r/Γ for both D_{CH} and D_{KLD} even if different boundary conditions are imposed.

Our results suggest the deviation from scaling for D_{CH} and D_{KLD} measures the impact of lateral boundaries (sidewalls) on the chaotic flow (Fig. 3). Sidewalls affect convection patterns due to the mismatch in the thermal conductivities of the sidewall and the fluid; sidewall effects have previously been probed primarily at small ϵ near convection onset [14, 18]. Here, we examine the effect of sidewalls far from onset by comparing the behavior of ρ for experiments with different sidewall conditions at $\epsilon = 0.8$. We see that ρ for both D_{CH} and D_{KLD} exhibits the same deviation from scaling for experiments in different sized convection cells, as long as the lateral boundary conditions are similar (experiments D-I, D-II and D-III in Fig. 3). However, in experiments where the (plastic) lateral boundaries increase sidewall forcing of the convective flow (D-IV in Fig. 3) ρ for both D_{CH} and D_{KLD} deviates from scaling at smaller r/Γ than for experiments with (paper) lateral boundaries where sidewall forcing is weaker (D-III in Fig. 3). More specifically, for both D_{CH} and D_{KLD}, ρ decreases by about 30% (from unity) at $r/\Gamma = 0.86d$ in D-I, D-II and D-III and at $r/\Gamma = 0.74d$ in D-IV. Moreover, our measurements are robust in the respect that nonlinearities associated with shadowgraph imaging do not alter our results; measurements of D_{CH} and D_{KLD}, computed for the full circular system and a circular region ($r = 15d$) from long time series of shadowgraph images, fluctuate only 3% and 10%, respectively, as the effective optical distance is varied over an order of magnitude in experiments [16].

Relating experimentally accessible measures of the number of DOF (e.g., D_{CH} and D_{KLD}) to more direct measures (e.g., D_λ) remains an open question. Recent direct simulations of RBC by Duggleby and Paul [12] yielded the relationship $D_{\mathrm{KLD}} \approx 19.7 D_\lambda$ from the variation of both dimensions with a range of system sizes $6 \leq \Gamma \leq 15$ in a cylindrical convection cell. Our results suggest that examining the effect of finite system size on D_λ may provide a way to link D_λ quantitatively to D_{CH} and D_{KLD}. In particular, it would be interesting to know whether ρ behaves in a universal fashion; i.e., to explore whether ρ associated with D_λ exhibits a similar functional dependence as that shown by D_{CH} and D_{KLD} in Fig. 3). In this regard, future studies that couple RBC laboratory experiments with numerical simulations with realistic boundary conditions at the same parameter values would be of greatest value.

This work is supported by the Department of Energy under Grant No. 97891.

[1] M. C. Cross and P. C. Hohenberg, Rev. Mod. Phys. **65**, 851 (1993).

[2] A. Wolf, J. B. Swift, H. L. Swinney, and J. A. Vastano, Physica D **16**, 285 (1985).

[3] D. Ruelle, *Turbulence, Strange Attractors, and Chaos* (World Scientific, Singapore, 1995).

[4] P. Manneville, Lecture Notes in Physics **280**, 319 (1994).

[5] D. A. Egolf and H. S. Greenside, Nature **369**, 129 (1994).

[6] D. A. Egolf, I. V. Melnikov, W. Pesch, and R. E. Ecke, Nature **404**, 733 (2000).

[7] M. R. Paul, M. I. Einarsson, P. F. Fischer, and M. C. Cross, Phys. Rev. E **75**, 045203 (2007).

[8] M. P. Fishman and D. A. Egolf, Phys. Rev. Lett. **96**, 054103 (2006).

[9] A. E. Deane and L. Sirovich, J. Fluid Mech. **222**, 231 (1991).

[10] S. M. Zoldi and H. S. Greenside, Phys. Rev. Lett. **78**, 1687 (1997).

[11] T. Kaczynski, K. Mischaikow, and M. Mrozek, *Computational Homology* (Springer-Verlag, Newyork, 2004).

[12] A. Duggleby and M. R. Paul, submitted to Computers and Fluids, arXiv:0905.4847v1 (2009).

[13] E. Bodenschatz, W. Pesch, and G. Ahlers, Annu. Rev. Fluid Mech. **32**, 709 (2000).

[14] J. R. de Bruyn, E. Bodenschatz, S. W. Morris, S. P. Trainoff, Y. Hu, D. S. Cannell, and G. Ahlers, Rev. Sci. Instrum. **67**, 2043 (1996).

[15] S. W. Morris, E. Bodenschatz, D. S. Cannel, and G. Ahlers, Phys. Rev. Lett. **71**, 2026 (1993).

[16] K. Krishan, H. Kurtuldu, M. F. Schatz, S. Madruga, M. Gameiro, and K. Mischaikow, Phys. Fluids **19**, 117105 (2007).

[17] S. M. Zoldi, J. Liu, K. M. S. Bajaj, H. S. Greenside, and G. Ahlers, Phys. Rev. E **58**, R6903 (1998).

[18] Y. Hu, R. Ecke, and G. Ahlers, Phys. Rev. E **48**, 4399 (1993).

[19] We could not perform experiments with CO_2 and the plastic in long observation times since it absorbs the gas and swells over time in high pressure [14]